ACTA ASTRONOMICA
Vol. **66** (2016) pp. 391–403

Variable Intensities of Molecular Features in the Spectrum of AE Aur

J. Krełowski[1], G. A. Galazutdinov[2,3,4], G. Mulas[5], A. Bondar[6], F. A. Musaev[4,7,8], A. Shapovalova[9], C. Cecchi-Pestellini[10], Y. Beletsky[11] and B.-C. Lee[12]

[1] Center for Astronomy, Nicholas Copernicus University, Grudziądzka 5, 87-100 Toruń, Poland
e-mail: jacek@umk.pl
[2] Instituto de Astronomia, Universidad Catolica del Norte, Av. Angamos 0610, Antofagasta, Chile
[3] Pulkovo Observatory, Pulkovskoe Shosse 65, Saint-Petersburg, 196140, Russia
[4] Special Astrophysical Observatory, Nizhnij Arkhyz, 369167, Russia
[5] Istituto Nazionale di Astrofisica – Osservatorio astronomico di Cagliari, Via della Scienza 5, 09047 Selargius (CA), Italy
[6] International Center for Astronomical and Medico-Ecological Research, Zabolotnoho Str. 27, Kiev, Ukraine
[7] Institute of Astronomy of the Russian AS, Pyatnitskaya st. 48, Moscow, 119017, Russia
[8] Terskol Branch of Institute of Astronomy of the Russian AS, Peak Terskol, 361605, Russia
[9] Ural Federal University, 51 Lenin st., Ekaterinburg, 620000, Russia
[10] Istituto Nazionale di Astrofisica – Osservatorio astronomico di Palermo, Piazza Parlamento 1, 90134 Palermo (PA), Italy
[11] Las Campanas Observatory, Carnegie Observatories, Casilla 601, La Serena, Chile
[12] Korea Astronomy and Space Science Institute 776, Daedeokdae-ro, Yuseong-gu, Daejeon 305-348, Korea

Received June 6, 2016

ABSTRACT

Using spectra of the star AE Aur (HD 34078), covering the period 1997–2015, we suggest that two strong molecular features of CH and CH^+ underwent detectable changes of intensity. In the last five years both CH and CH^+ declined sharply and systematically, with the CH/CH^+ ratio steadily growing. No variations in the radial velocities of the observed interstellar features was detected during the covered period.

Key words: *ISM: lines and bands – ISM: general*

1. Introduction

For a long time interstellar spectral lines observed in absorption on the spectra of background stars were considered as being necessarily of constant intensity:

given the spatial (cloud size) and time (interstellar chemistry and physics) scales. Both intrinsic changes – in column densities of line carriers and geometric changes in the line-of-sight, due to the relative motion of observer and background star – were deemed to be negligible during an astronomer's life. By the end of 90s, however, it became clear that interstellar clouds are not homogeneous, but may contain structures on much smaller scales, *e.g.*, Deshpande (2000), Smith *et al.* (2013). Some intensity variations of the features originated in them may therefore be observable on human time scales (Crawford *et al.* 1994, 1998).

Also radio observations using high angular resolution led to the discovery of tiny-scale variations of atomic structures (Stanimirović *et al.* 2010). Recently Dirks and Meyer (2016) reported the evidence of temporal variability in the interstellar NaI absorption toward HD 47240 which lies behind the Monoceros Loop supernova remnant (SNR). Eight-year period spectral observations reveal significant variation in both the observed column density and the central velocities. Authors suggest this variation would imply ≈ 10 a.u. fluctuations within the expanding SNR shell. Rao *et al.* (2016) reported dramatic disappearance of strong NaI D component toward three stars in the direction of the Vela supernova remnant.

In particular, some variability may be detectable as the line-of-sight toward a background source sweeps through different parts of the intervening clouds, if large proper motions are involved. The most likely candidate objects to observe this effect are expected to be bright, because large proper motions typically characterize nearby stars. The modeling of possible phenomena in the interstellar medium was proposed in several papers, *e.g.*, Hennebelle and Audit (2007) which may allow understanding the situation inside some relatively small scale interstellar clouds.

Herbig (1999) proposed AE Aur as an object with a sufficiently large proper motion to possibly see measurable variations of interstellar features on a scale of a few years. This O9.5V star, of apparent *V* magnitude about 6, is moving across the line-of-sight with a speed of 43 mas per year (Boissé *et al.* 2009). At an estimated distance of ≈ 500 pc (Humphreys 1978, Megier *et al.* 2009) this corresponds to a linear speed transversal component of 22 a.u. per year. If the density structures in the intervening cloud are of the a.u. size, this may be sufficient to cause some detectable variations of intensities and radial velocities (*RV*s) of interstellar lines or bands with time. However, Herbig (1999) found no such variations of *RV*s comparing his spectra from 1998 to those of Adams (1949). His *RV*s are only marginally higher than the former ones, with a difference compatible with measurement errors.

The problem of intensity variations of interstellar features in the spectrum of AE Aur was addressed subsequently by a number of studies. Rollinde *et al.* (2003), using observations from several instruments collected over about a decade, found that while the assumption of constant equivalent widths (*EW*s) was marginally compatible with their CH and CH^+ measurements, they hinted some real variability. Using their highest resolution spectra, they also fitted the unresolved structure in both features with three velocity components, two narrow ones and a broad, shallow

one. Even in the highest resolution spectra, the features are unresolved, showing only a slight asymmetry and shallow wings, so the authors cautiously remark that the fit solution is not unique. More recently, Boissé *et al.* (2005) detected the presence of highly excited H_2 along the line-of-sight, with no measurable variability over a few years in FUSE data. This was interpreted as evidence of intense interaction of AE Aur with the molecular cloud it is traversing, as also hinted by the presence of an apparent bow shock in Spitzer observations at 24 μm (France *et al.* 2007). The latter authors also showed that the amount of dust inferred from scattered light accounts for only a small fraction (a few tenths of a magnitude) of the observed A_V toward AE Aur, the rest being due to the colder foreground translucent cloud. Moreover, Boissé *et al.* (2009) observed evident CO emission centered at the star, using the IRAM 30-m telescope. Very recently, Gratier *et al.* (2014) combined the former single-dish observations with complementary ones obtained with the Plateau de Bure interferometer, resolving the foreground CO emission in two dense "globulettes", with angular sizes around $4''$ and estimated number densities just below 10^5 cm^{-3}. These "globulettes" are found to have radial velocities compatible with those of the two sharp components of CH and CH^+ fitted by Rollinde *et al.* (2003), and together should produce a visible extinction of about 0.3 mag along the line-of-sight toward AE Aur, out of its total $A_V \approx 1.6$ mag. Such cloudlets are reminiscent of those found serendipitously by Heithausen (2002).

The molecular features available to ground based optical observations are extremely intense in the spectra of this star, proving a sort of peculiarity of the interstellar material obscuring it. This overabundance is even more outstanding if one assumes that CH and CH^+ do not originate in the translucent cloud producing the bulk of the extinction in the line-of-sight, but instead only in the part directly interacting with the star, as proposed by Boissé *et al.* (2009) and Gratier *et al.* (2014). Even the nature of the shock front ahead of AE Aur is uncertain: Boissé *et al.* (2009) found its distance from the star inconsistent with the estimated stellar wind, and Ochsendorf *et al.* (2014) proposed that the observed emission arc at 24 μm may actually be due to dust swept up by radiation pressure ahead of the actual shock front between stellar wind and the ambient cloud. On the other hand, López-Santiago *et al.* (2012) detected conspicuous X-ray emission from the arc, hinting that a bow shock is actually present.

In this work we present new observations of this interesting line-of-sight, that together with other previously collected, strongly suggest systematic variations in the intensity of both CH and CH^+ transitions that declined systematically, with the CH/CH^+ ratio steadily growing, in the past few years.

2. Observations

The list of spectra of HD 34078 that we analyzed covers almost 20 years, *i.e.*, dates back to 1997 (Table 1).

T a b l e 1

CH, CH^+ and CaII K line measurements

date	CH^+ 4232 Å				CH 4300 Å				CaII K		Julian day	facility
	integrated		profile fit		integrated		profile fit		integrated			
	EW	Δ*EW*	*EW*	Δ*EW*	*EW*	Δ*EW*	*EW*	Δ*EW*	*EW*	Δ*EW*	2 450 000	
1997–11–14	43.9	2.2	41.8	2.6	51.3	2.2	50.4	3.1	125.5	0.5	766.5	Terskol[a]
1997–11–19	49.1	2.5	46.3	4.4	55.6	2.7	55.4	4.0	131.0	0.6	771.5	Terskol[a]
2004–02–05	44.4	0.6	45.2	1.0	53.8	0.7	52.7	0.7	134.5	1.5	3040.5	BOES
2004–03–07	45.2	0.5	45.9	1.0	54.2	0.8	52.7	1.0	133.4	1.5	3071.5	BOES
2004–08–27	47.8	0.8	45.0	0.9	55.7	0.8	52.0	0.8	129.8	1.5	3244.5	Terskol[b]
2005–12–18	41.4	0.9	41.5	0.9	51.3	0.9	50.4	0.9	133.2	1.1	3447.5	UVES
2005–04–03	45.4	1.3	43.6	1.3	54.6	1.3	51.5	1.3	132.8	3.3	3463.5	Terskol[b]
2005–04–06	47.5	1.2	44.8	1.1	52.6	1.1	52.6	1.1	125.5	3.7	3466.5	Terskol[b]
2005–04–13	45.9	1.1	43.3	1.2	54.4	1.1	54.4	1.1	131.0	2.6	3473.5	Terskol[b]
2006–10–07	43.8	0.7	42.3	0.9	54.3	0.9	52.8	0.6	136.5	2.2	4015.5	BOES
2007–12–04	46.8	2.1	46.1	2.7	55.5	2.8	54.3	2.9	133.9	2.7	4439.5	Terskol[a]
2008–01–16	45.6	0.6	46.0	0.8	55.3	1.5	54.1	1.2	131.5	1.8	4481.5	Terskol[a]
2008–02–01	48.3	0.5	48.3	0.5	56.6	0.5	56.6	0.5	133.6	1.0	4497.5	BOES
	47.7	0.6	47.7	0.6	56.6	0.5	56.6	0.5	133.6	1.3	4497.5	BOES
2008–02–02	47.8	0.8	47.8	0.8	55.5	0.6	53.4	0.7	133.6	1.3	4498.5	BOES
	46.9	0.7	47.0	0.9	55.8	0.5	53.3	0.7	134.4	1.3	4498.5	BOES
2010–12–24	45.0	0.7	45.3	1.3	51.4	0.6	51.6	1.6	129.2	1.1	5554.0	Terskol[a]
2011–01–13	44.8	1.2	42.1	1.8	52.4	1.2	52.8	1.8	129.5	4.1	5574.5	Terskol[a]
2011–12–14	38.0	1.7	37.6	2.3	50.0	1.8	49.2	2.1	127.0	3.1	5909.5	Terskol[a]
2011–12–29	40.7	1.4	37.7	1.7	52.1	1.8	50.8	1.8	130.7	2.7	5924.5	Terskol[a]
2012–01–06	38.3	0.7	38.6	1.8	49.8	1.1	50.2	2.4	133.0	3.2	5932.0	Terskol[a]
2012–01–12	37.1	0.5	37.7	0.5	52.1	0.4	49.1	0.3	131.8	1.0	5938.5	MIKE
2013–11–15	37.0	1.5	34.7	1.4	53.4	1.4	49.1	1.3	131.5	2.3	6611.5	HARPS–N
2014–03–14	32.4	2.3	33.8	2.3	45.6	1.6	46.6	2.0	128.0	2.2	6730.5	Terskol[a]
2014–08–17	30.5	0.9	32.5	1.5	45.1	0.7	44.5	1.6	123.3	4.5	6887.5	Terskol[a]
2014–09–09	32.6	0.7	32.4	1.0	50.5	0.9	48.1	1.2	132.7	2.8	6910.5	MIKE
2014–10–08	31.6	1.2	31.4	1.8	46.5	1.3	45.9	1.7	122.0	2.0	6938.5	Terskol[a]
2014–12–26	32.6	2.7	32.9	2.9	44.4	1.5	43.7	2.8	133.0	4.4	7017.5	Terskol[a]
2015–01–13	31.5	1.9	31.0	2.2	45.0	1.4	44.1	2.0	129.1	3.7	7035.5	Terskol[a]
2015–01–14	30.8	1.5	30.1	2.1	46.8	1.6	45.4	1.6	127.2	3.7	7036.5	Terskol[a]
2015–10–30	29.9	0.5	29.8	0.5	45.8	0.6	44.9	0.9	130.8	1.0	7326.3	BOES

(a) $R = 45\,000$; (b) $R = 120\,000$.

The bulk of data were collected at the ICAMER (North Caucasus, Russia) observatory, with the aid of the coudé echelle spectrograph MAESTRO (Musaev *et al.* 1999) fed by a 2-m telescope. These spectra have been obtained in two operating modes of the instrument, with resolving powers respectively of $R = 45\,000$ and 120 000. MAESTRO in $R = 45\,000$ mode provides a complete spectrum (≈ 95 spectra orders) in the range $\approx 3500-10\,100$ Å in a single exposure made with the aid of Wright Instruments CCD camera equipped with a 1242×1152 matrix (pixel size 22.5×22.5 μm). In $R = 120\,000$ mode the CCD covers some 40% of the complete spectrum, though CH, CH^+ and CaII K can be recorded simultaneously. Typical signal-to-noise (S/N) ratios of MAESTRO's spectra are $\approx 70-100$ and $\approx 100-150$ for $R = 45\,000$ and $R = 120\,000$ modes, respectively.

One spectrum in the range 3050–10 400 Å was obtained at the ESO Paranal observatory, with the UVES spectrograph (Dekker *et al.* 2000) mounted on the Nasmyth focus of the 8-m VLT-UT2 telescope; the resolution near the molecular features is $R \approx 50\,000$ corresponding to the applied slit width $1.''0$, and the S/N ratio ≈ 250.

One spectrum was taken with the HARPS-N spectrograph (Cosentino *et al.* 2012) – a copy of the HARPS spectrograph at the ESO La Silla Observatory – installed at the TNG at La Palma Island (Canary Islands). Spectrum covers the 383–690 nm wavelength range with the resolving power $R \approx 115\,000$, and the S/N ratio ≈ 100.

Two spectra were acquired with the MIKE spectrograph (Bernstein *et al.* 2003) fed by the 6.5-m Magellan telescope at Las Campanas observatory (Chile). Spectra were observed with a $0.''35 \times 5''$ slit. We estimated the resolving power using the solitary Thorium lines. It is $\approx 56\,000$ ($\Delta v \approx 5.4$ km/s) on the blue branch (3600–5000 Å) of spectrograph. The recorded spectra are averages (in the pixel space) of 24 (the resulting S/N ratio reaches $\approx 400-800$) and 7 ($S/N \approx 100-200$) individual exposures for 2012 and 2014 runs respectively.

Lastly, our sample includes eight spectra obtained through the fiber-fed echelle spectrograph BOES (Kim *et al.* 2007) installed on the 1.8-m telescope at the Bohyunsan Observatory (South Korea). In all cases the spectrograph allows us to record a whole spectral range from ≈ 3500 to $\approx 10\,000$ Å divided into 75–76 spectral orders. The spectrograph has three observational modes providing the resolving power of $R = 30\,000$, 45 000, and 90 000. Our 2004's spectra (S/N ratio varies in the range) are in the lowest one, 2006's are of $R = 45\,000$ and, spectra collected in 2008 are of $R = 90\,000$. In all spectra S/N ratio varies in the range $\approx 200-400$ depending on the wavelength.

All spectra were processed in a standard way using both IRAF (Tody, 1986) and our own DECH[1] codes. The wavelength scale of all spectra was aligned to the interstellar rest wavelength position using the CH 4300 Å line.

All measurements have been performed with the aid of DECH code. Equivalent widths error were estimated using the Eq.(7) from Vollmann and Eversberg (2006) which do include contributions from both photon noise and continuum uncertainties.

3. Results

In Table 2 we compare equivalent widths and *RV* data from Herbig (1999) with our own, acquired using the BOES spectrograph in two epochs.

The EWs of atomic lines coincide within the measurement errors in both sets of observations, with the exception of KI 4044 Å lines. The intensity ratio of the components of this doublet can be easily determined by means of standard atomic

[1] *http://gazinur.com/DECH-software.html*

T a b l e 2

Equivalent widths and radial velocities of interstellar lines from Herbig (1999), BOES(2004) and BOES(2015)

Feature [Å]	*EW*(Her) [mÅ]	*EW*(2004) [mÅ]	*EW*(2015) [mÅ]	*RV*(Her) [km/s]	*RV*(2004) [km/s]	*RV*(2015) [km/s]	ratio[a]
FeI 3859.911	10.2 ± 1.0	4.6 ± 0.6	6.0 ± 0.6	15.6	14.6	15.6	1.30
CN 3874.607	11.4 ± 0.4	10.4 ± 0.8	10.1 ± 1.1	13.4	13.9	14.4	0.97
CH 3878.774	7.7 ± 0.6	6.9 ± 0.6	6.2 ± 0.7	15.2	14.7	15.4	0.90
CH 3886.410	22.2 ± 2.2	18.8 ± 1.1	15.3 ± 0.8	15.3	14.6	14.8	0.81
CH 3890.217	13.2 ± 2.6	13.0 ± 1.0	10.9 ± 0.7	14.9	14.8	14.4	0.84
CaII K 3933.664	130.0 ± 0.6	132.8 ± 1.4	131.0 ± 1.1	14.7	13.9	14.4	0.99
CH^+3957.692	27.3 ± 0.4	29.7 ± 0.9	18.7 ± 0.6	15.5	14.7	14.7	0.63
CaII H 3968.470	79.0 ± 3.0	79.9 ± 1.2	82.2 ± 0.9	15.0	14.1	14.7	1.03
KI 4044.143	9.4 ± 0.4	6.0 ± 1.0	4.4 ± 0.6	11.5	12.7	11.8	0.73
CaI 4226.728	8.0 ± 2.2	6.6 ± 0.6	6.2 ± 0.5	15.6	15.7	16.5	0.94
CH^+4232.548	47.0 ± 0.4	45.2 ± 0.5	29.9 ± 0.5	15.3	14.6	14.4	0.66
CH 4300.313	58.0 ± 0.2	54.2 ± 0.8	45.8 ± 0.6	15.3	14.5	14.8	0.85
KI 7698.965	–	179.9 ± 1.7	173.7 ± 1.2	–	15.6	15.6	0.97

[a]Strength ratios: 2015/2004.

theory, and it should be close to 2 for unsaturated lines, decreasing somewhat in case of saturation. Since the value inferred from Herbig (1999) data is about 8.5, the reported EW may be wrong for any of these lines. Our molecular lines are generally weaker than Herbig's ones. Our *RVs* are a bit blue-shifted for all stronger lines, except for those of CaI and CaII which have evident Doppler structure. Some difference between *RV*'s of CaII lines and molecular features was mentioned by Adams (1949). Our values reported in Table 2 refer to the radial velocities that bring the center of the strongest Doppler component observed to the reference laboratory wavelength, corrected for the heliocentric reference frame.

Our spectra cover the period 1997–2015. Naturally some of them are of better, some of worse quality. We have selected two spectra from the BOES spectrograph in evidently different epochs: 2004 and 2015. The first spectrum was acquired before the decline of molecular features started, the second is very recent. The comparison is given in Fig. 1 and in Table 2. The result is shown in Fig. 1. It compares three CH and two CH^+ lines. It is evident that the CH features considered are weaker in the most recent spectrum. On the other hand both CH^+ lines: 3957 Å and 4232 Å are strongly weaker in the same spectrum. This may suggest that the ratio of the features is variable and can be different in more recent observations. It is important to mention that interstellar CaII, CaI and KI lines are of the same intensity in both spectra as well as stellar lines.

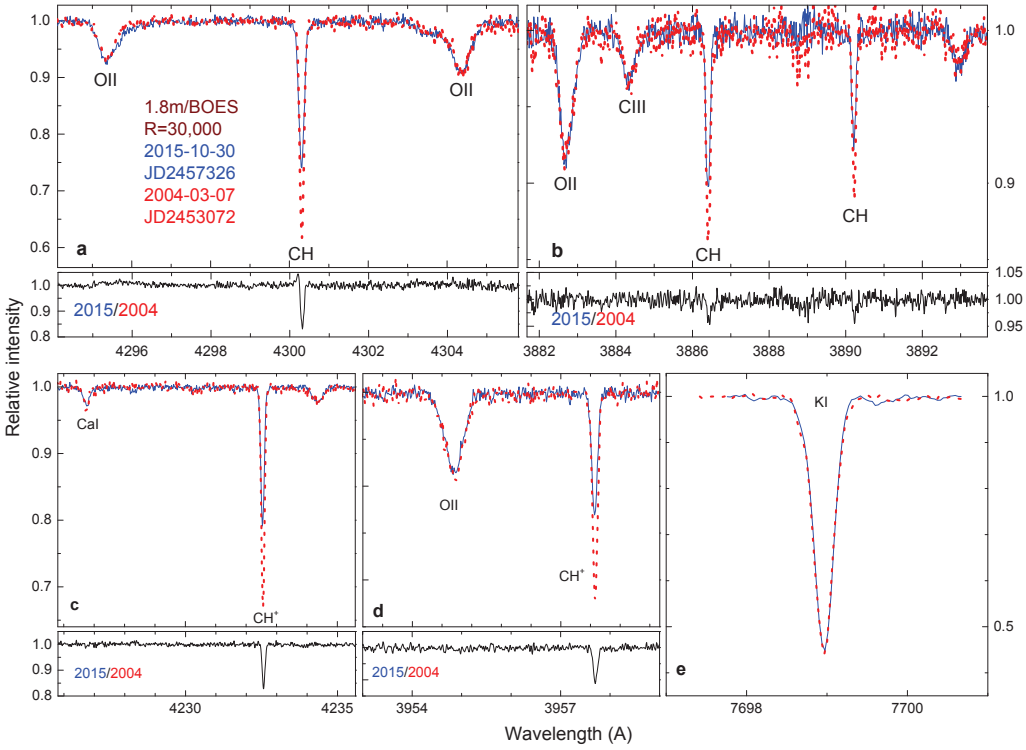

Fig. 1. Comparison between observations made in different epochs using the same instrument. Molecular lines are evidently weaker in the recently recorded spectrum in a sharp contrast to stellar lines and the interstellar CaI and KI ones.

We focus on the strongest features, *i.e.*, CH^+ 4232 Å and CH 4300 Å, for quantitative comparisons of EWs. The molecular features at 3886 Å and 3957 Å are much weaker, making their measurements more uncertain. Moreover, the $B-X$ 3886 Å CH line lies on the wing of a strong HI stellar line, making the definition of its local continuum level difficult, and thus adding to the uncertainty in its measurement. Still, the behavior of the weaker features, when examined in the spectra with the highest S/N ratio, is entirely consistent with that of the stronger ones (see Fig. 1). We devoted an extreme care to the definition of the continua over the measured lines. Visual inspection of heavily saturated absorption lines, *e.g.*, the NaI doublet, shows that their flat bottom coincides with zero flux, within noise. This rules out significant uncorrected scattered light contamination in any of the spectrographs used, which would instead result in some residual flux at the bottom of saturated lines. In the case of the CH^+ 4232 Å line, which is blended with a stellar line, the de-blending procedures available in IRAF and the DECH software were applied.

The CH^+ 4232 Å and CH 4300 Å lines are only mildly saturated, as seen in our highest resolution data and also in Rollinde *et al.* (2003), with their even

higher resolution $R = 170\,000$. The lack of saturation follows the Doppler splitting, demonstrated in the latter paper. For these two features, therefore, equivalent widths were obtained both *via* direct integration and by profile fitting. The profile fitting routines of the DECH code were used to match the observed profiles with the minimum number of Doppler components (typically three) that reduced the residual to the noise level. The integrated area of the best fitting sum was used as the measure of the equivalent width. While our data are compatible with the *RV* components obtained by Rollinde *et al.* (2003), the fitting solutions are highly non unique. This is fully expected, given that the separation in radial velocity determined by Rollinde *et al.* (2003) for the narrow components is about ≈ 2 km/s, with velocity dispersions of the order of 3 km/s, while our highest resolution is only slightly less than 3 km/s. Even in Rollinde *et al.* (2003) the fit is clearly stated to be non unique, in spite of their higher spectral resolution. Indeed the narrow components are not resolved also in Rollinde *et al.* (2003), that inferred their presence only from the asymmetry of the observed profile. In any case, as long as profiles are adequately fitted, the total area of any resulting blend of components is insensitive to the ambiguity in how the intensity is distributed among the components. One can therefore still use profile fitting as a reliable method to measure the equivalent width, along with direct integration. As to the CaII K line, being it more heavily saturated we only measured its equivalent width by direct integration.

The relation between the measured intensities and epoch of observation for both molecular features is given in Fig. 2. It is evident that a nearly constant (inside the measurement errors) intensities of molecular features are followed by a rather sharp decline starting around 2009, and still ongoing. This does not depend on the instrument used. The decline is greater for CH^+ than for CH. The lines shown in the top and middle panels of Fig. 2 represent the result of a least-squares fit of the data with two lines: a horizontal one up to time T_B and a decreasing line from T_B on. The free parameters of this fit are the constant height of the horizontal line, the break time T_B, and the intercept and angular coefficient of the decreasing line. The fit is made both with our data only (green line), and including also the OHP-SOPHIE and McDonald data points from Boissé *et al.* (2009 – blue line). Both CH and CH^+ yield a T_B around year 2009. The inclusion of the best data from Boissé *et al.* (2009) does not appear to change significantly the fit results. There appears to be some real scatter around the best fitting lines, even if only slightly larger than formal errors.

The CaII K line only shows some apparently random oscillations, even if somewhat larger than its formal uncertainty. Its EW always remains close to the one reported by Herbig (1999), *i.e.*, 130 mÅ.

Conversion to column densities may be done making use of the scaling relations given in Boissé *et al.* (2009), Eqs.(1–2), with the cautionary remark that such column densities depend on the admittedly non unique decomposition in radial velocity components in Rollinde *et al.* (2003).

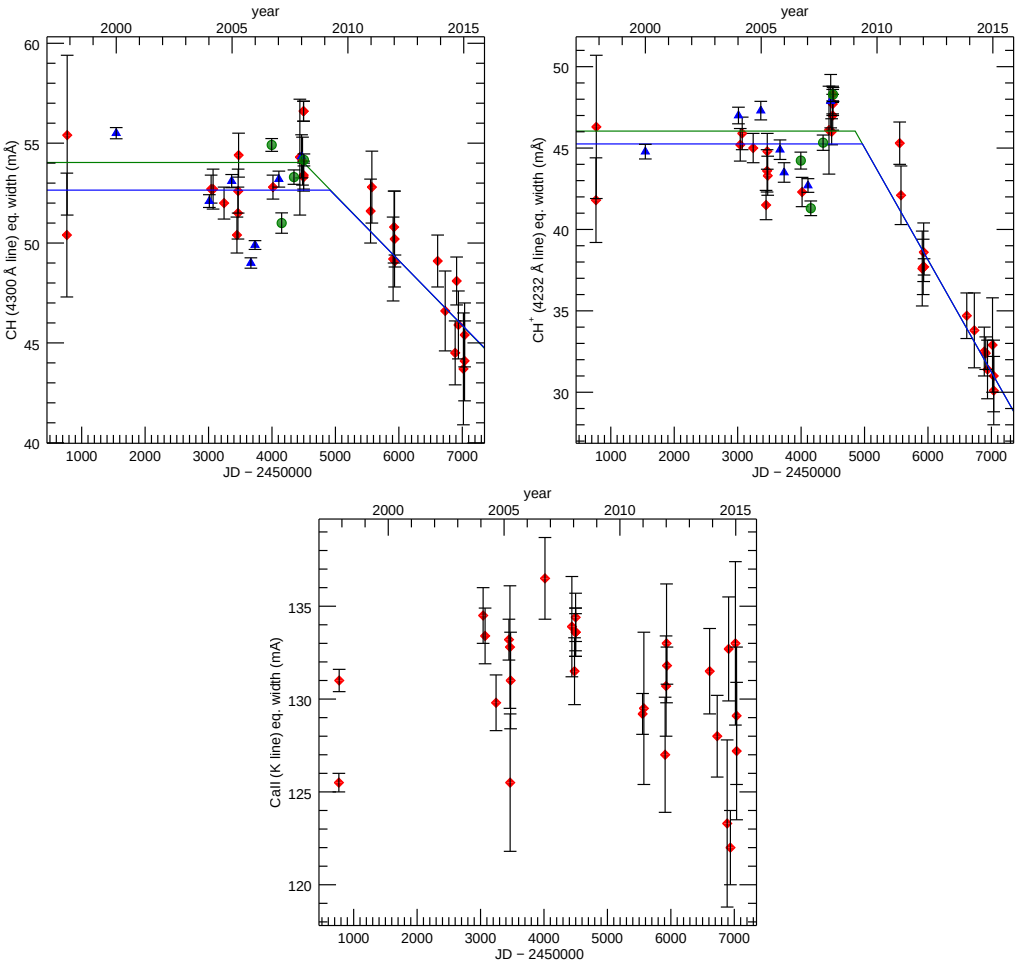

Fig. 2. CH 4300 Å, CH^+ 4232 Å, and CaII K line intensities plotted as a function of the observation epoch (in Julian days). The CH^+ decline is evident while that of CH is smaller. Red dots are our measurements, blue dots and green dots are respectively McDonald and OHP–SOPHIE observations, both from Boissé *et al.* (2009).

We also examined the correlation between the measured EWs, shown in Fig. 3. In all plots we show the best fitting straight line through the data. The correlation among CH and CH^+ EWs is astonishingly good ($R \approx 0.9$) in our data and OHP-SOPHIE data from Boissé *et al.* (2009), with all of them being within one or two standard deviations from the best fitting line. Only some McDonald data points, also from Boissé *et al.* (2009), appear to stand prominently out of the correlation. This may depend either on their smaller error, meaning that the correlation breaks down at very high accuracy, or that their errors are underestimated. The top right and bottom panels of Fig. 3 show the correlation of CH and CH^+ EWs with that of CaII. In this case there can possibly be some loose correlation, but variations are at the noise level, so this is inconclusive.

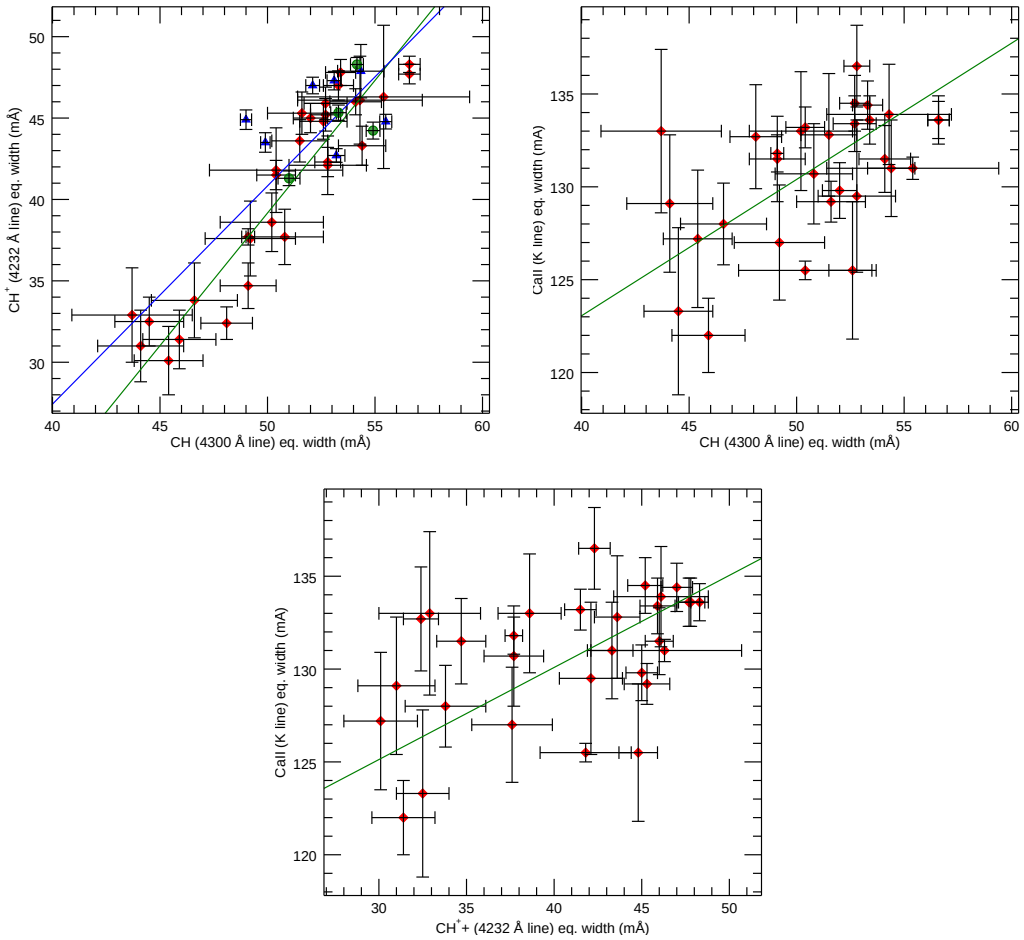

Fig. 3. Correlation plots of the EWs of CH, CH^+ and CaII. *Left top panel:* CH *vs.* CH^+; *right top panel:* CH *vs.* CaII; *bottom panel:* CH^+ *vs.* CaII. The green line in *all panels* is the best fitting straight line for our data. The blue line on *top panel* is the best fitting line including in the fit also McDonald and OHP–SOPHIE data from Boissé *et al.* (2009).

4. Discussion and Conclusions

Our HARPS-N spectrum, with its highly reliable wavelength calibration, indicates a heliocentric *RV* of ≈ 15 km/s for most interstellar spectral features. However, something very interesting is visible in this spectrum. In Fig. 4 we show that an evident Doppler structure exists in the interstellar CaII and NaI lines, but quite surprisingly the molecular CH and CH^+ lines do not match the *RV* of any of the resolved CaII and NaI Doppler components.

The CH and CH^+ lines that we measured do not show resolved radial velocity structure at the resolution of our data. They are compatible with two unresolved components at the radial velocities of the two cloudlets found by Gratier *et al.*

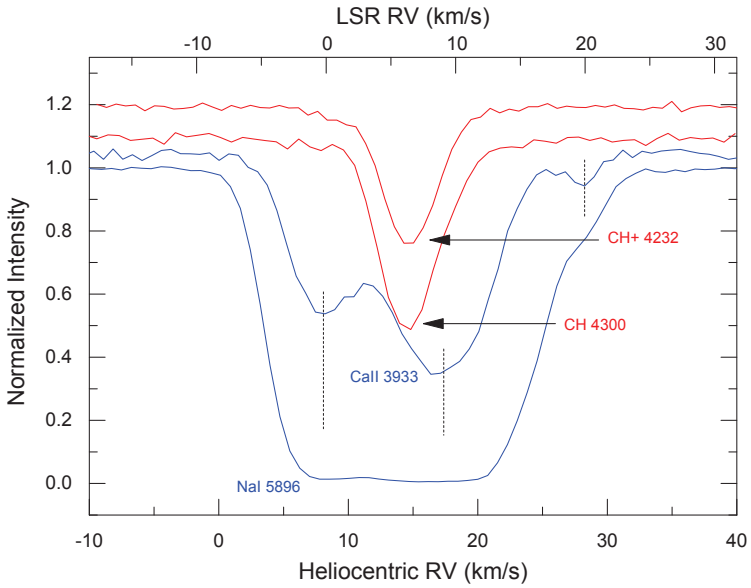

Fig. 4. Doppler structure of some interstellar lines, seen in HARPS-N (November 2013) spectrum of AE Aur. Atomic features are in blue, molecular ones in red. Different lines are slightly vertically displaced to make them more distinguishable. Vertical lines mark the central radial velocities of the resolved Doppler components in the CaII 3933 Å profile.

(2014), as well as with the (substantially matching) non unique decomposition solution found by Rollinde *et al.* (2003). If NaI and CaII coexist with CH and CH^+, their features must be weak, and thus blended with other stronger components, indistinguishable from them at this resolving power. At least the molecular features do not share radial velocities with the evident, strong Doppler components of CaII and NaI. Our data do not show any trend of change with time in the *RVs* for all of the interstellar lines observed in the spectrum of AE Aur. It is interesting that in all datasets the lines of iron show the largest *RVs* and that all molecular lines exhibit the same *RVs*. Our new spectrum from BOES, compared with the old one (from 2004) shows that radial velocities of KI lines are systematically larger than those of CH or CH^+. Unfortunately the resolution of BOES is too small to resolve even the CaII lines and thus it is difficult to say whether KI share any of the well-resolved Doppler of H and/or K line.

It has been long recognized that the ISM is not in an equilibrium state, *i.e.*, interstellar clouds cannot be treated as closed systems. The basic problem for the chemistry is how to incorporate the ambient oxygen and carbon into molecules. Oxygen is ionized by slow charge transfers with H^+, while the abundant ion C^+ does not react rapidly with H_2. Chemistry may thus proceed by endothermic reactions $C^+ + H_2 \rightarrow CH^+ + H$ ($\Delta E/k \approx 5000$ K) and $O + H_2 \rightarrow OH + H$ ($\Delta E/k \approx 3000$ K). CH may be formed through both cold and warm chemistries (Zsargó and Federman 2003). This is consistent with the moderate decline of CH line intensities as compared to those of CH^+, if indeed chemistry proceeds through non-equilibrium

routes. This may explain the observed correlation between CH and CH^+ EWs, with CH consisting of a "warm" part forming together with CH^+ and a remaining part of "cold" CH, forming through uncorrelated chemical channels, resulting in the non-zero intercept of the best-fitting correlation line.

Summing up, the systematic decline, which has been ongoing for about six years, indicates a sharp drop of the total column density intersected by the line-of-sight, on a spatial scale of a few hundred a.u.

Acknowledgements. This paper includes data gathered with the VLT and UVES spectrograph, with the 3.5 m Telescopio Nazionale Galileo and HARPS-N spectrograph, with the BOES spectrograph at the 1.8 m telescope at Bohyunsan Optical Astronomy Observatory (South Korea), with the 2 m telescope at ICAMER and the MAESTRO spectrograph, and with the 6.5 m Magellan telescope at Las Campanas and the MIKE spectrograph. JK acknowledges the financial support of the Polish National Center for Science during the period 2015-2017 (grant 2015/17/B/ST9/ 03397). GAG thanks the Russian Science Foundation (project 14-50-00043, the Exoplanets program) for support of observational and interpretational parts of this study. AS was supported by The Ministry of Education and Science of the Russian Federation within the framework of the research activities (project 3.1781.2014/K). GM and CCP acknowledge the support of the Autonomous Region of Sardinia, Project CRP 26666 (Regional Law 7/2007, Call 2010).

REFERENCES

Adams, W.S. 1949, *ApJ*, **109**, 354.
Bernstein, R., Shectman, S.A., Gunnels, S.M., Mochnacki, S., and Athey, A.E. 2003, *Proc. SPIE*, **4841**, 1694.
Boissé, P., Le Petit, F., Rollinde, E., Roueff, E., Pineau des Forets, G., Andersson, B.-G., Gry, C., and Felenbok, P. 2005, *A&A*, **429**, 509.
Boissé, P., *et al.* 2009, *A&A*, **501**, 221.
Cosentino, R., *et al.* 2012, *SPIE Conf. Ser.*, **8446**, 1.
Crawford, I.A., Spyromilio, J., Barlow, M.J., Diego, F., and Lagrange, A.M. 1994, *MNRAS*, **266**, 65.
Crawford, I.A., Beust, H., and Lagrange, A.M. 1998, *MNRAS*, **294**, 31.
Dekker, H., D'Odorico, S., Kaufer, A., Delabre, B., and Kotzlowski, H. 2000, *SPIE Conf. Ser.*, **4008**, 434.
Deshpande, A.A. 2000, *MNRAS*, **317**, 199.
Dirks, C., and Meyer, D.M. 2016, *ApJ*, **819**, 45.
France, K., McCandliss, S.R., and Lupu, R.E. 2007, *ApJ*, **655**, 920.
Gratier, P., Pety, J., Boissé, P., Cabrit, S., Lesaffre, P., Gerin, M., and Pineau des Forêts, G. 2014, *A&A*, **570**, 71.
Hennebelle, P., and Audit, E. 2007, *A&A*, **465**, 431.
Herbig, G.H. 1999, *PASP*, **111**, 809.
Heithausen, A. 2002, *A&A*, **393**, L41.
Humphreys, R. M. 1978, *ApJS*, **38**, 309.
Kim, K.-M., *et al.* 2007, *PASP*, **119**, 1052.
López-Santiago, J., *et al.* 2012, *ApJ*, **757**, L6.
Megier, A., Strobel, A., Galazutdinov, G.A. and Krełowski, J. 2009, *A&A*, **507**, 833.

Musaev, F.A., Galazutdinov G.A., Sergeev A.V., Karpov N.V., and Podyachev Yu.V. 1999, *Kinematics Phys. Celest. Bodies*, **15**, 216.
Ochsendorf, B.B., Cox, N.L.J., Krijt, S., Salgado, F., Berné, O., Bernard, J.P., Kaper, L., and Tielens, A.G.G.M. 2014, *A&A*, **563**, 65.
Rao, N.K., Muneer, S., Lambert, D.L., and Varghese, B.A. 2016, *MNRAS*, **455**, 2529.
Rollinde, E., Boissé, P., Federman, S.R., and Pan, K. 2003, *A&A*, **401**, 215.
Smith, K.T., Fossey, S.J., Cordiner, M.A., Sarre, P.J., Smith, A.M., Bell, T.A., and Viti, S. 2013, *MNRAS*, **429**, 939.
Stanimirović, S., Weisberg, J.M., Pei, Z., Tuttle, K., and Green, J.T. 2010, *ApJ*, **720**, 415.
Tody, D. 1986, *Proc. SPIE*, **627**, 733.
Vollmann, K., and Eversberg, T. 2006, *Astron. Nachr.*, **327**, 862.
Zsargó, J. and Federman, S.R. 2003, *ApJ*, **589**, 319.